

## CONTACTLESS MEASURING METHOD OF BLADE VIBRATION DURING TURBINE SPEED-UP

Pavel Procházka, František Vaněk, Jan Cibulka, Vítězslav Bula\*

*A novel method of contactless measurement of turbine blade vibration during increasing (decreasing) operational speed is presented. The method is based on evaluation of time differences of blade passages along contactless sensors placed on the stator, and substitutional data correction using a numerical model. The method has been verified both numerically and experimentally. For the experimental research on the bladed model wheel of the Institute of Thermomechanics and subsequent applications under operating conditions, two new types of sensors functioning on magnetoresistive and induction principle have been developed.*

Keywords: rotor blade vibration, contactless measurement, tip-timing

### 1. Introduction

Measurement system VDS-UT (Vibrodiagnostic System UT) has been recently developed in the Institute of Thermomechanics of the Academy of Sciences of the Czech Republic for contactless measurement of turbine blade vibration [1], [4], [5], [6]. This system has been focused on the analysis of vibration of steam turbine blades operating at a constant rotor speed. The aim of presented research work was to design and verify on an experimental model a new method for contactless measurements of transient phenomena, when natural frequencies of blades with large vibration amplitudes may be significantly excited (e.g. by passing critical speed during turbine speed-up). Measurements at irregular rotation of the machine required changes in both sensing and evaluating units of the vibrodiagnostic system. New algorithms based on a comparison of separate blade deflections with an original state (etalon) enable to detect changes in vibration characteristics of blades and thus their possible damage due to an inappropriate operational regime or material defects.

### 2. The numerical model

Information on regimes of turbine speed-up has been obtained from several power plants, and also measurements by means of the storage oscilloscope Yokogawa DL750 were performed, to establish the maximal value of a turbine speed acceleration. The measurements evaluated and information received indicate that the turbines accelerate to the operational speed with practically constant angular acceleration, ranging up to  $10 \text{ rad s}^{-2}$ . The typical course of turbine speed-up in time can be seen in Fig.1. Two constant horizontal sections represent warming-up time delays. Turbine rotational speed increases linearly under electronic control. A uniformly accelerated rotational motion has been presumed for the numerical model.

---

\* Ing. P. Procházka, CSc., Ing. F. Vaněk, CSc., J. Cibulka, Ing. V. Bula, Institute of Thermomechanics AS CR, Dolejškova 5, 182 00 Praha 8, Czech Republic

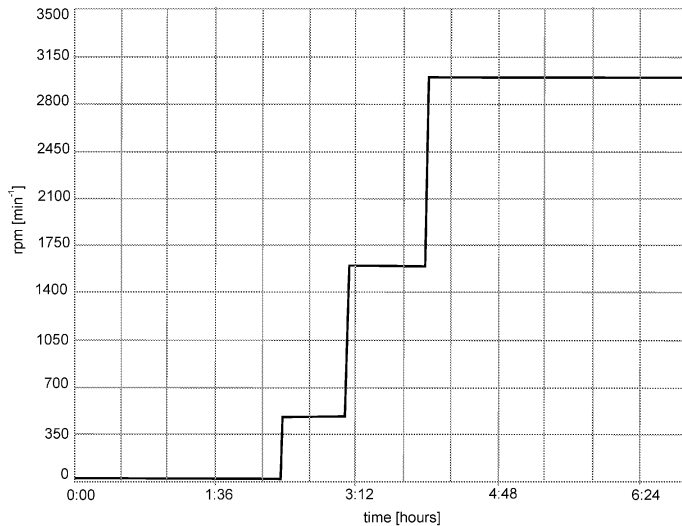


Fig.1: A sample record of turbine speed-up acceleration

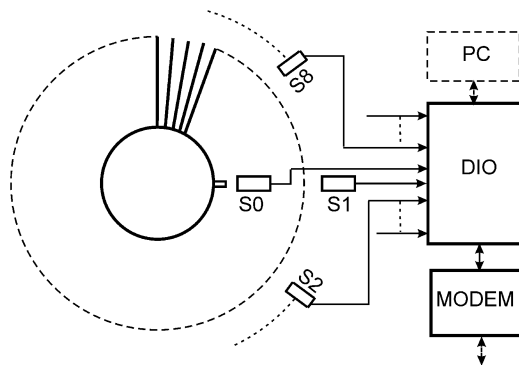


Fig.2: Block diagram of the contactless vibrodiagnostic system

A block diagram of the 8-channel vibrodiagnostic system can be seen from in Fig. 2. The contactless sensors S1 to S8 placed on the stator generate impulse signals by passages of each turbine blade tip. The sensor S0 detects the passages of a magnetic reference mark attached to the shaft.

Impulse output signals of the sensors S0 to S8 are digitized and connected to the central measuring unit DIO. This unit includes a precise counter and, as the result, a numerical value of time is assigned to each generated pulse. The time data complemented by a sensor address and auxiliary operational analogue readouts are sent to a local or distant (via modem or net) computer (PC). Time differences of each blade passage are calculated and transferred to circumferential deflections and subsequently to blade bending deflections. Using the algorithm of DFT, the amplitudes and frequencies of vibration of all blades can be ascertained. This method is often referred as tip-timing.

A numerical model has been developed to simulate contactless sensing and evaluation process of rotor blade vibration, when increasing or decreasing the turbine speed. The numerical model was implemented in the program environment TestPoint 6.1. Considering uniform approaching the operational speed 3000 rpm of real turbines, a uniformly accele-

rated rotational motion of the rotor with a constant angular acceleration is assumed in the mathematical model. The basic equation of the motion can be expressed as

$$\sigma = \omega_0 t + \frac{\alpha t^2}{2}, \tag{1}$$

where  $\sigma$  [rad] is the angular distance,  $\omega_0$  [rad s<sup>-1</sup>] is the angular velocity for  $t = 0$ ,  $t$  [s] is time and  $\alpha$  [rad s<sup>-2</sup>] is the angular acceleration. Assuming contactless sensors equally spaced around the perimeter of the stator, we get for the angular distance of the  $j$ -th sensor,  $j = 1, 2, \dots, n_s$

$$\sigma = \frac{2\pi}{n_s} j. \tag{2}$$

Solving equation (1), we obtain the real root for the time of the blade passage around the  $j$ -th sensor

$$t_s = \frac{-\omega_0 + \sqrt{\omega_0^2 + \frac{4\pi \alpha}{n_s} j}}{\alpha}. \tag{3}$$

The numerical model is based on this solution. The interactive control panel of the numerical model can be seen in Fig. 3. The program allows entering parameters of blade vibration (frequency, amplitude and phase shift of two main components of bending vibration in the circumferential direction), an instantaneous state of the turbine (initial speed, angular acceleration) and the vibrodiagnostic system (number of contactless sensors on the stator and their angular distance).

The model can take into account failure of a sensor as well. The example in Fig. 3 simulates the state of the vibrodiagnostic system with 7 functioning sensors and one sensor out

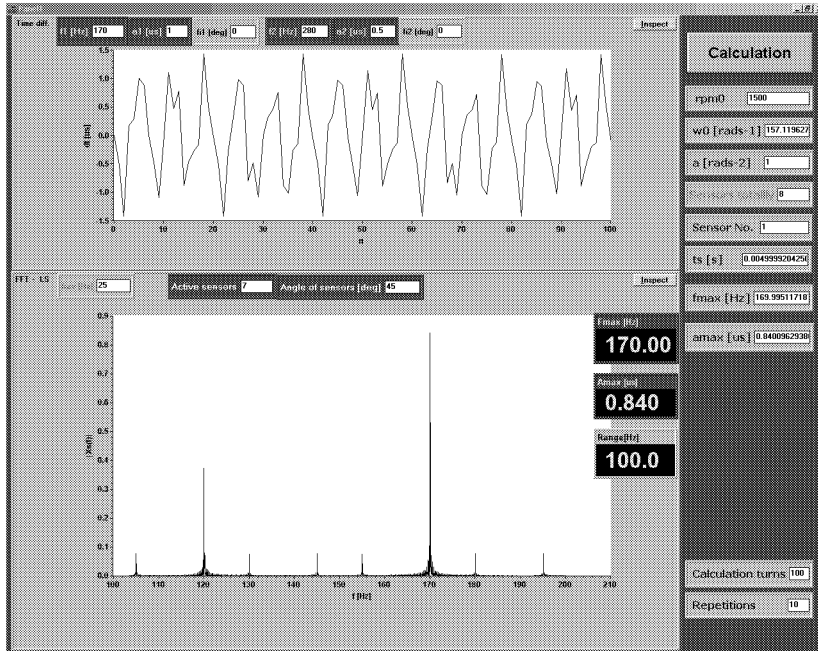


Fig.3: The control panel and the display of the numerical model

of order. A uniform distribution of sensors along the perimeter of the stator is assumed. The corresponding sequence of samples of time differences, which is the input for the discrete Fourier transform (DFT), is compiled from data generated by the modelled passage of blades along contactless stator sensors (upper graph). The output of the model is the linear amplitude spectrum of time differences of vibrating blades during uniformly accelerated rotational motion of the rotor (lower graph). The numerical values of the frequency and the amplitude of the main spectral function component are displayed. The result of the calculation provides further auxiliary information, e.g. range of the spectrum, initial angular velocity  $\omega_0$  and the time of the blade passage along a given sensor. Appropriate measuring method can be designed and optimised by this numerical model, permitting thus utilization of this method for precise measurements during turbine speed acceleration.

Features of contactless vibrodiagnostic systems based on the method of time differences were analysed for a wide range of angular acceleration (from 0.01 to 2000  $\text{rads}^{-2}$ ). For the rotational speed varying from 100 rpm to 3000 rpm, the impact of angular acceleration on the frequency and amplitude of blade vibrations was examined. For these calculations, natural frequencies of 130, 150 and 170 Hz were chosen, as they correspond to the real values of natural frequencies of the long blades of low-pressure turbine stages, e.g. in power stations Pruněřov and Temelín. Examples of dependence obtained by the numerical model calculations for 500, 1500 and 3000 rpm are shown in Figs.4 to 10. While the frequency

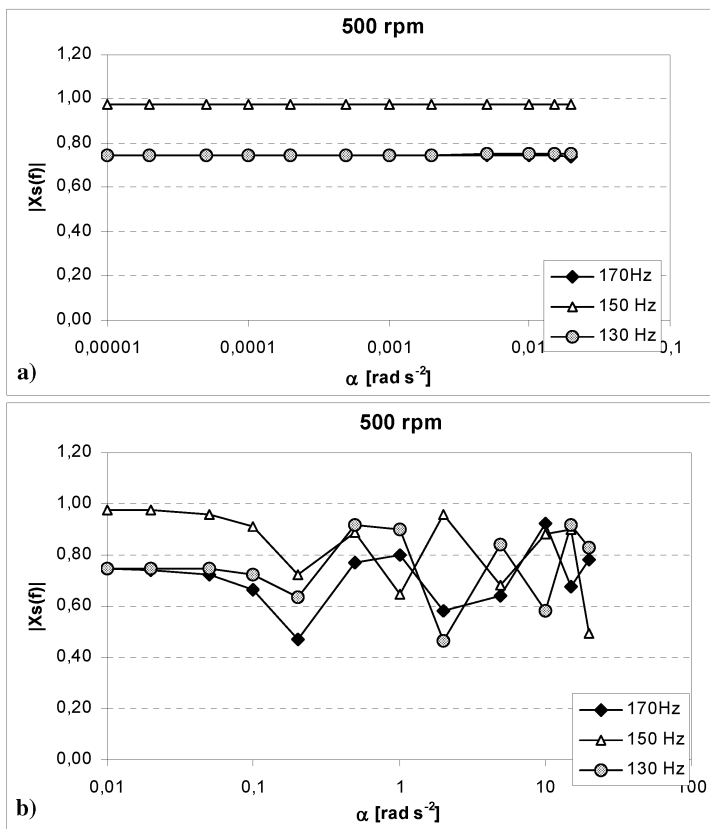


Fig.4: The maximal value of the amplitude spectral function of blade vibration in dependence on the angular acceleration  $\alpha$  for the rotor speed of 500 rpm

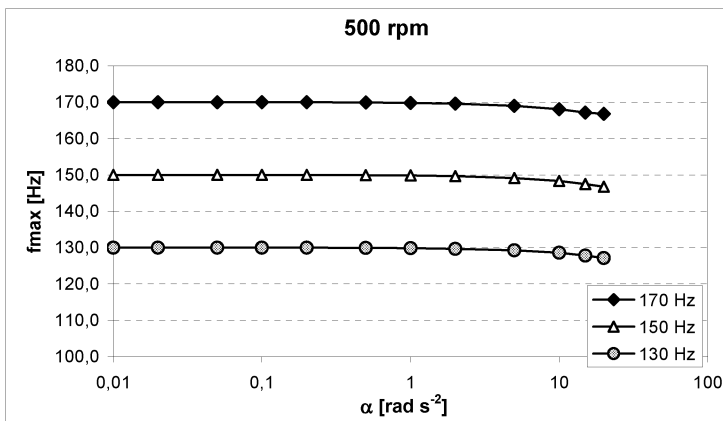


Fig.5: The dependence of the calculated dominant frequency of blade vibration on the angular acceleration  $\alpha$  for the rotor speed of 500 rpm

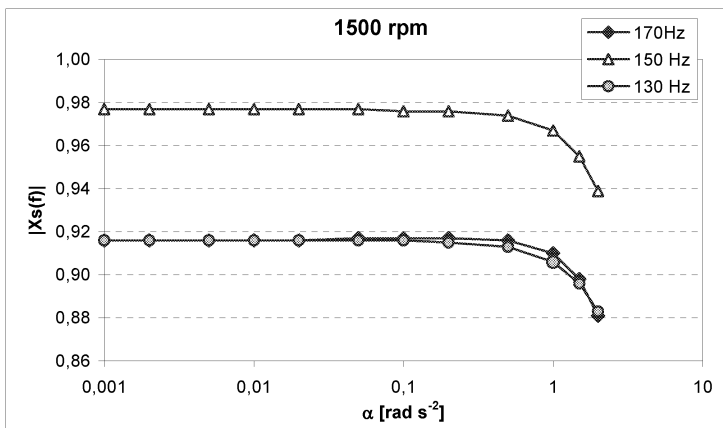


Fig.6: The maximal value of the amplitude spectral function of blade vibration in dependence on the angular acceleration  $\alpha$  for the rotor speed of 1500 rpm

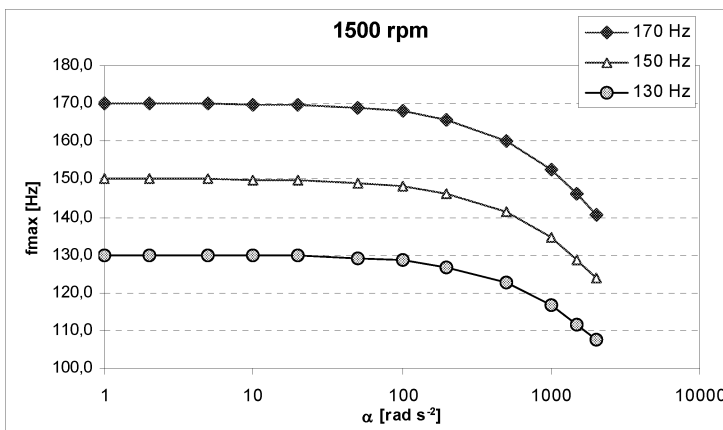


Fig.7: The dependence of the calculated dominant frequency of blade vibration on the angular acceleration  $\alpha$  for the rotor speed of 1500 rpm

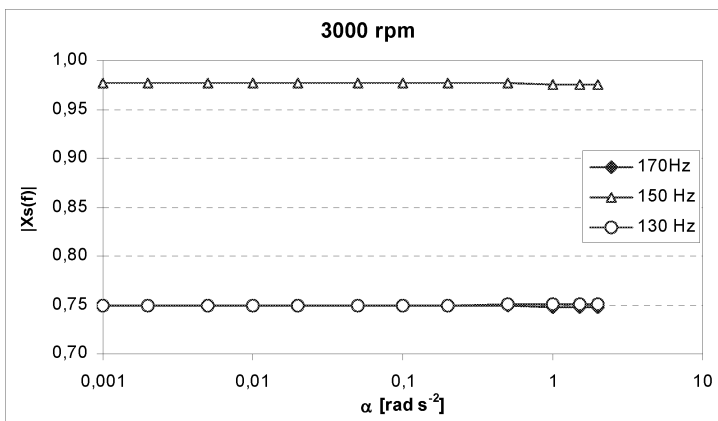


Fig.8: The maximal value of the amplitude spectral function of blade vibration in dependence on the angular acceleration  $\alpha$  for the rotor speed of 3000 rpm

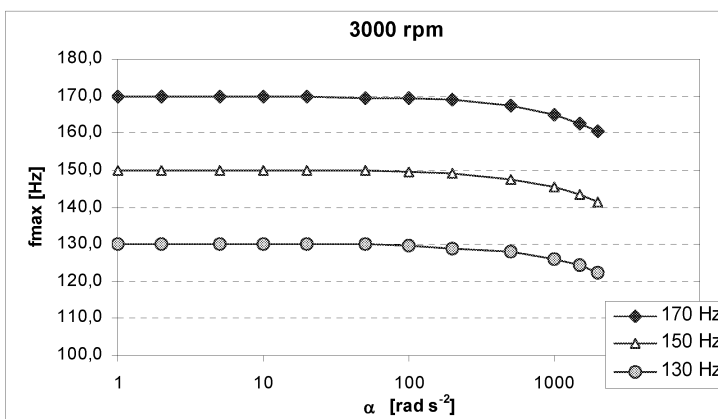


Fig.9: The dependence of the calculated dominant frequency of blade vibration on the angular acceleration  $\alpha$  for the rotor speed of 3000 rpm

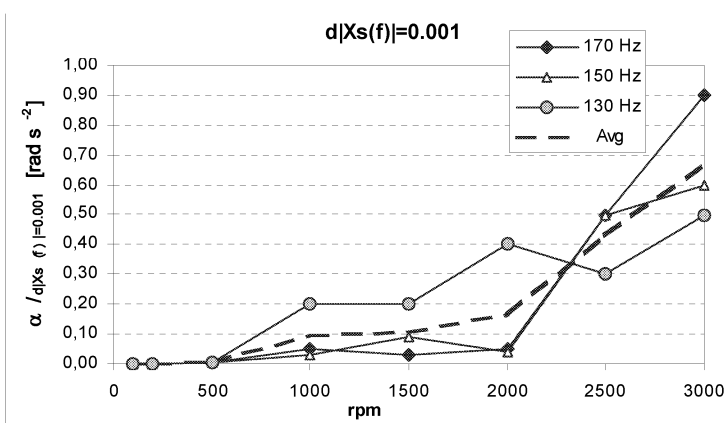


Fig.10: The value of angular acceleration  $\alpha$  resulting in the decrease  $d|X_s(f)| = 0.001$  of the maximum of the amplitude spectrum in dependence on rpm

error pertains to the values of angular acceleration  $\alpha > 10 \text{ rad s}^{-2}$ , the amplitude error is already discernible at  $\alpha > 0.01 \text{ rad s}^{-2}$ . For higher values of  $\alpha > 1 \text{ rad s}^{-2}$ , we can observe a decreasing character of the amplitude spectral function verging to a chaotic character. This effect is caused by the properties of DFT.

The dependence of the angular acceleration  $\alpha$  resulting in the decrease  $d|X_s(f)| = 0.001$  of the amplitude spectrum maximum on rpm can be seen from Fig. 10. Sensitivity to the value of acceleration depends on the instantaneous rotor speed. For low values of the rotor speed, already small values of acceleration  $\alpha$  can cause relatively large changes of the maximum of the amplitude spectral function of blade vibration. The amplitude error due to these changes decreases with the rotor speed. Hence, the limit for a fixed amplitude decrease ( $d|X_s(f)| = 0.001$  for example in Fig. 10) increases with increasing rotor speed. Similar curves can be observed for the frequencies 130, 150 and 170 Hz. The dashed line shows an average curve.

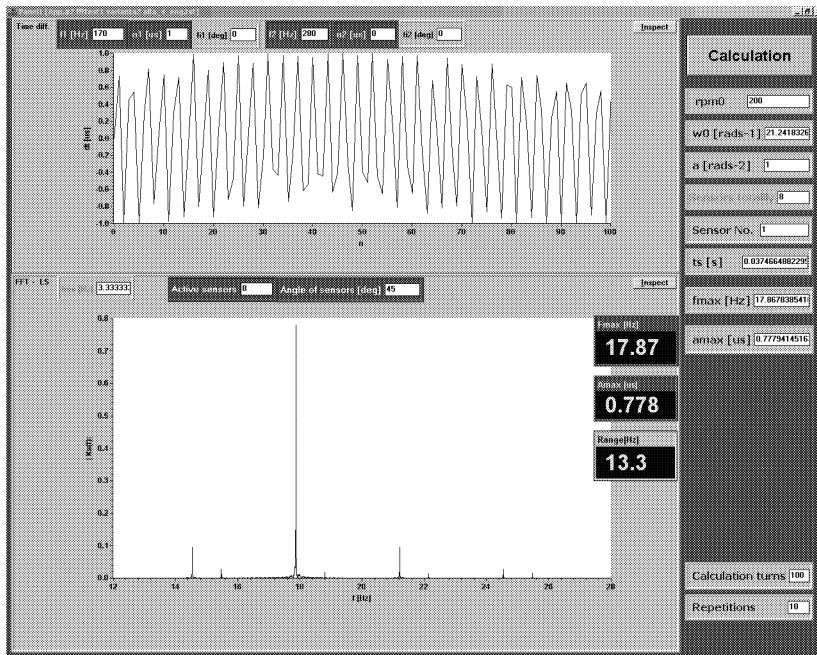


Fig.11: Emergence of the side bands by 200 rpm and  $\alpha = 1 [\text{rad s}^{-2}]$

Based on the knowledge obtained from the numerical modelling, a substitutional method for correcting measurement errors caused by acceleration of the machine has been proposed. At first, initial rotor speed is ascertained by a precise time measurement of passages of magnetic marks placed on the rotor. Similar method is used to determine acceleration of the rotor. Subsequently, the value of acceleration is put to zero and primary approximate characteristics of blade vibration are calculated. Then, assuming a constant average value of real acceleration, the obtained values are entered to the numerical model, which yields correct data. This method enables measuring even at high angular acceleration values, when the results would be greatly distorted by large amplitude and frequency errors.

Increasing the angular acceleration at high rotational speed or decreasing rotational speed at higher values of a constant angular acceleration, we can observe phenomena of formation

of side bands in the amplitude spectral function. An example of this situation is displayed for 200 rpm and  $\alpha = 1 \text{ [rad s}^{-2}\text{]}$ . Even if the number of active sensors  $n_s = 8$  is maximal and single spectral line is expected, we can observe several additional spectral lines shifted by the frequency  $f_{\text{rot}} = 3.33 \text{ [Hz]}$ . This value represents the initial value of the rotational frequency given as

$$f_{\text{rot}} = \frac{\text{rpm}}{60} , \tag{4}$$

whereas  $R$  is the range of the DFT

$$R = n_s f_{\text{rot}} . \tag{5}$$

In the given example  $R = 26.67 \text{ Hz}$ . The higher side bands are mirror flipped at the frequency band limits. The input frequency of blade vibrations  $f_1 = 170 \text{ [Hz]}$  is transformed by the given value of the sampling rotational frequency to  $f_{1t} = 16.67 \text{ [Hz]}$ . Due to the frequency error, this value is distorted to the real output  $f_{1o} = 17.87 \text{ Hz}$ .

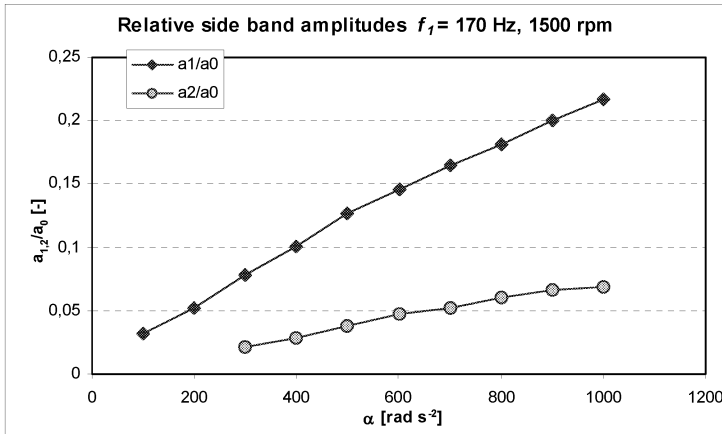


Fig.12: Relative amplitudes of the first and second side bands to the amplitude of the main spectral line  $a_0$  in dependence on an angular acceleration  $\alpha$  for 1500 rpm

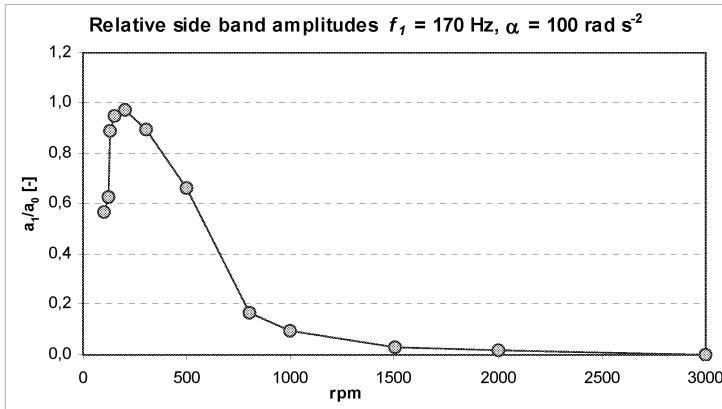


Fig.13: Relative amplitudes of the first side band to the amplitude of the main spectral line  $a_0$  in dependence on rpm for  $\alpha = 100 \text{ rad s}^{-2}$  and  $f_1 = 170 \text{ Hz}$

Occurrence of side bands has been studied for a wide range of rotational speed from 100 to 3000 rpm. The dependence of the relative amplitude of the first and second side bands  $a_1/a_0$  and  $a_2/a_0$ , respectively, for the speed 1500 rpm and the vibration frequency 170 Hz can be seen in the example in Fig. 12.

Assuming a fixed angular acceleration  $\alpha$  we can study the dependence of the ratio of the side band amplitude and of the appropriate maximum of the spectral amplitude function. An example of the dependence of the relative side band amplitude on the rotor speed is shown in Fig. 13. The curve is characterized by a maximum around 200 rpm and a falling course with increasing speed.

### 3. Experimental verification of the method

For the experimental verification of the method, two new types of blade passage sensors have been developed and both static and dynamic characteristics of these sensors have been verified. Special emphasis was placed on the resilience and endurance of these sensors, so that they could be utilized under real operational conditions. The sensors were used in the contactless vibrodiagnostic system VDS-UT at the power station Temelín. For protection of intellectual property associated with the development of new types of sensors, patent applications [2], [3] have been submitted for registration.

Both inductive and magnetoresistive sensors developed for sensing a position of rotating machine parts operate as contactless sensors located on the machine stator. The magnetoresistive sensors provide increased linearity and accuracy, and feature optimum direction of magnetization and the symmetry of the output signal. Current supplied sensors can measure their own internal temperature as well. Magnetoresistive sensors can be used for measurements by the circumferential speeds up to 700 m/s and ambient temperatures up to 200 °C. The construction of the sensor prevents water erosion. The photograph of the magnetoresistive sensor is shown in Fig. 14.

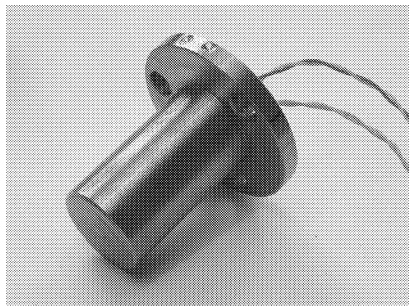
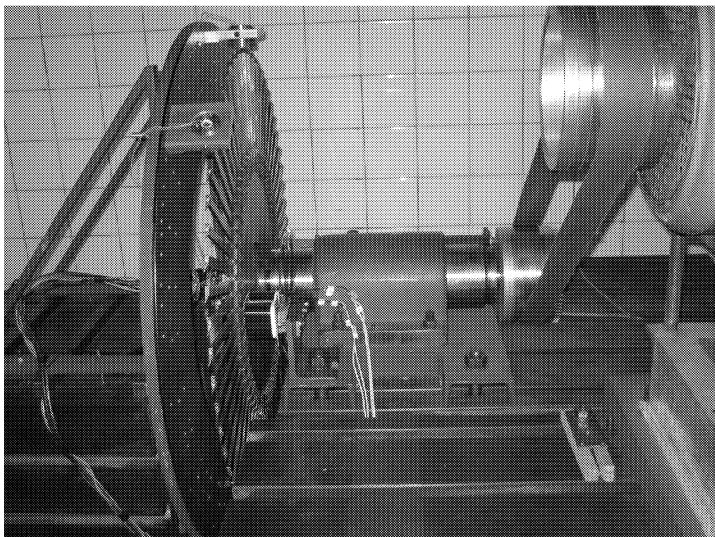


Fig.14: A contactless magnetoresistive sensor

The function of the modified arrangement of the vibrodiagnostic system for measuring during wheel speed-up and slow-down has been verified. Experiments were carried out on the experimental model of the bladed wheel fitted with 47 prismatic blades in the dynamic laboratory of the Institute of Thermomechanics. Necessary adjustments of regulation circuits of the wheel had been performed, which allowed uniform increase of the wheel speed in the range from 0 to 720 rpm with an angular acceleration from 0.01 to 1 [rad s<sup>-2</sup>]. To calibrate the proposed measuring method, existing strain gauge system of the model wheel was utilized. The arrangement of the model wheel can be seen in Fig. 15.

Examples of measurements performed on the model wheel during its uniformly accelerating speed from 0rpm to 720rpm are presented in Figs. 16 and 17 showing the records taken by the memory oscilloscope Yokogawa DL750. Channel 1\_FZ shows the signal of the reference phase mark, channel 2\_TL1 shows voltage output of a strain gauge located on the blade No. 1, channel 4\_MR shows voltage output of the contactless magnetoresistive sensor MR1 and channel 6\_60l shows the output of an auxiliary reference blade signal. The disk of the wheel was excited by a magnetic field of an alternating electromagnet with constant frequency of 60 Hz.



*Fig.15: The experimental model of the bladed wheel in the dynamic laboratory*

It can be observed from the signal envelope of the strain gauge in channel 2\_TL1 that by increasing the speed, initially the first mode shape and in the following section also the second mode shape are subsequently excited. While blade vibration is apparent from the amplitudes of the strain gauge signal, the corresponding information can be obtained from the output signal of the contactless magnetoresistive sensor using data processing method of time or amplitude differences.

A more detailed record involving one revolution of 627 rpm can be seen in Fig. 17. The strain gauge resonant signal is apparently modulated by a close harmonic signal. The trace 4\_MR shows impulses generated by passages of single blades. From amplitude and time changes of these impulse signals, the static and dynamic characteristics of blade vibration can be evaluated.

Calculating the linear amplitude spectra of the strain gauge signal and the magnetoresistive sensor signal by the software Viewer by Yokogawa, we can draw conclusions regarding character of vibration of the examined bladed wheel. Results of FFT calculations for 420 rpm in Fig. 18 show the dominant frequency of the amplitude spectrum of the magnetoresistive sensor 61 Hz, which corresponds to the frequency of the exciting signal of the electromagnet. The dominant frequency of the amplitude spectrum of the strain gauge signal is shifted down by the frequency of rotation  $f_{\text{rot}} = 7$  Hz, which indicates excitation of a forward wave.

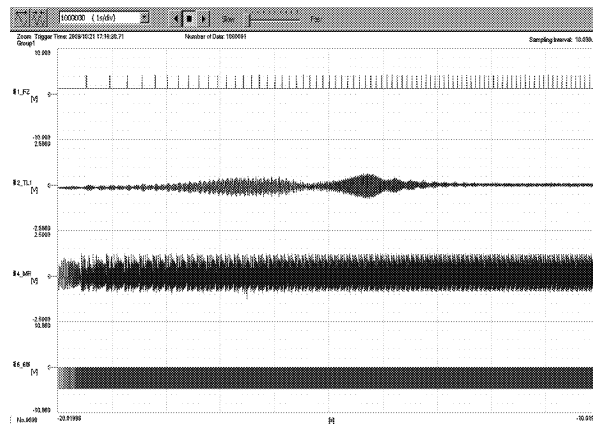


Fig.16: Measurements of uniformly accelerated rotation from 0 rpm to 720 rpm on the experimental model wheel recorded by a storage oscilloscope

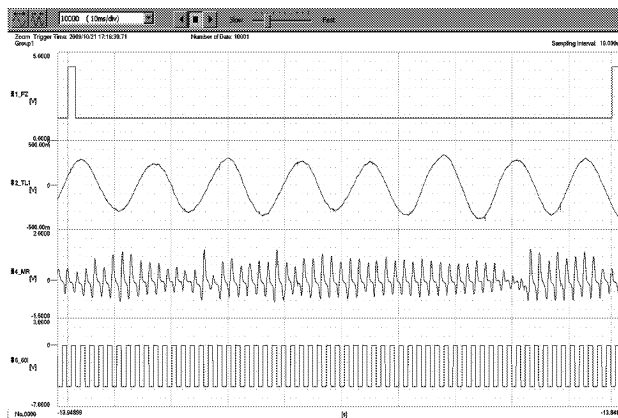


Fig.17: Measurement of uniformly accelerated rotation from 0 rpm to 720 rpm on the experimental model wheel recorded by the storage oscilloscope Yokogawa DL750. More detailed record of one revolution by 627 rpm

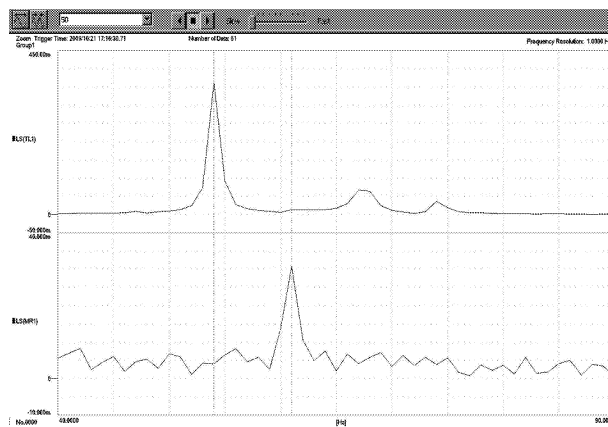


Fig.18: Linear amplitude spectra by 420 rpm (7 Hz) with dominant frequencies of LS(TL1) : 54 Hz, 68 Hz, 74 Hz and LS(MR1) : 61 Hz

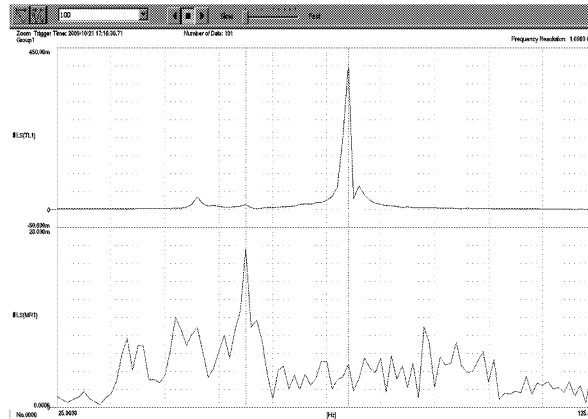


Fig.19: Linear amplitude spectra by 590 rpm (9.8 Hz) with dominant frequencies of LS(TL1) : 51 Hz, 61 Hz, 79 Hz and LS(MR1) : 61 Hz

In the second resonant range with higher rotational speed, the reverse frequency shift, leading to the higher value of the strain gauge dominant frequency compared to the excitation frequency, proves excitation of a backward wave (Fig. 19).

As results from the numerical modeling, negligible frequency errors occurred in the interval  $\alpha = \langle 0.01, 1 \rangle$  of the values of the angular acceleration adjustable on the experimental model. Consequently, only amplitude errors are measurable. Measured values were compared with the values calculated by means of the numerical model for speed ranging from 250 to 720 rpm. Examples of measured a calculated dependence of the relative amplitude of vibration on an angular acceleration  $\alpha$  for 250, 500 and 720 rpm can be seen in Figs. 20a), 20b) and 20c), respectively. The axial deflections of prismatic blades of the wheel model were converted into the radial direction by the angle edges of the blades (see Fig. 15). The amplitudes are related to the maximum values of the amplitude spectral function. From these diagrams, a good agreement of the experiment with the numerical modeling is apparent.

#### 4. Conclusion

Possibilities and restrictions of contactless measurements of vibration characteristics of turbine blades during increasing or decreasing operational turbine speed have been determined.

Modelling numerically contactless vibrodiagnostic process and assuming uniformly accelerated rotational movement, characteristics of a contactless measurement system based on the method of time differences were analysed for a wide range of values of angular acceleration  $\alpha$  from 0.001 to 2000  $\text{rad s}^{-2}$ . The influence of variation of the angular acceleration on the resulting values of frequency and amplitude of blade vibration was investigated for the speed range of 100 rpm to 3000 rpm.

Based on the numerical modelling, a substitution method for correcting errors caused by a non-zero rotor angular acceleration has been suggested. First, the initial rotational speed is ascertained by a precise time measurement of passages of magnetic marks placed on the rotor. Then, the same procedure is used to determine an instantaneous acceleration of the rotor. Subsequently, characteristics of blade vibrations are calculated for the rotation without acceleration. Then, assuming a constant average value of real acceleration, the

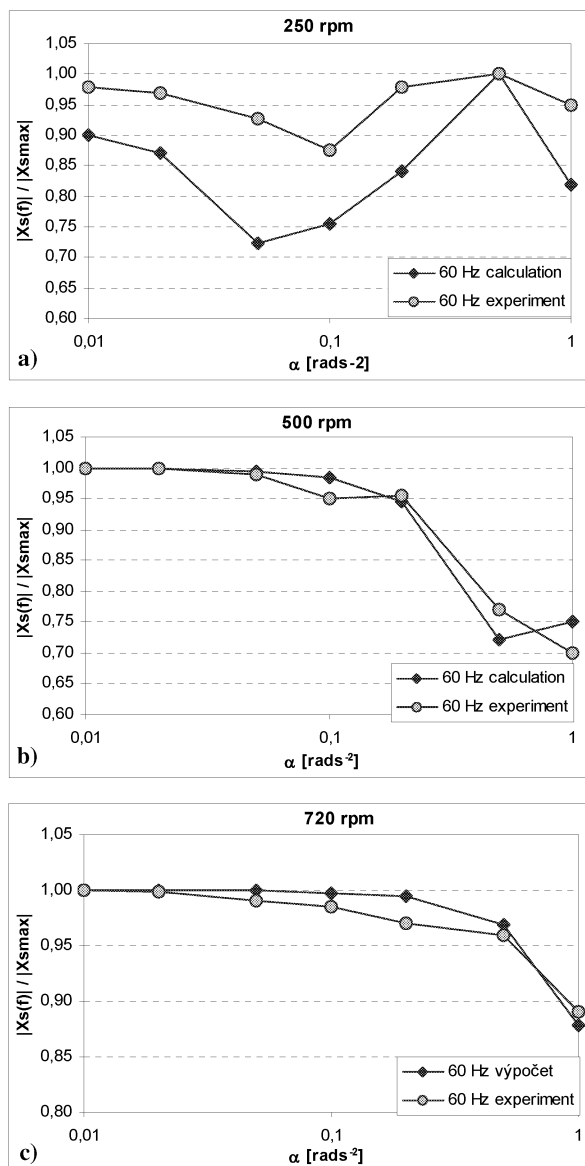


Fig.20: Relative amplitude of vibration of the blade No. 1 on angular acceleration  $\alpha$  for a) 250, b) 500 and c) 720 rpm. Output of the numerical model and measurement on the experimental model wheel of the Institute of Thermomechanics

obtained values are entered to the numerical model and original values are substituted by corrected data. This method enables measuring even at high angular acceleration values when the results would be normally distorted by large amplitude and frequency errors.

Verification of suggested measuring method was carried out on the model of the rotating bladed wheel in the dynamic laboratory of the Institute of Thermomechanics. Arrangement of modified vibrodiagnostic system has been proved for speed-up and slow-down regimes. Experiments were carried out for speeds from 0 to 720 rpm with a uniform acceleration  $\alpha$

ranging from 0.01 to 1 [rad s<sup>-2</sup>]. For the experiments, two new types of blade passage sensors have been developed and their static and dynamic characteristics have been verified. Magnetoresistive sensors feature extremely rapid dynamic response, which allows precise measurements even by peripheral speeds up to 700 [m/s]. High resilience and endurance of these sensors enables their usage in operational conditions at real power plants. The sensors were applied in the contactless vibrodiagnostic system VDS-UT installed at the power station Temelín.

### Acknowledgement

The research was supported and carried out within the pilot project of the research plan No. AV0Z20760514 of the Institute of Thermomechanics.

### References

- [1] Procházka P., Vaněk F., Pešek L., Cibulka J., Vaněk P.: An improvement of the vibrodiagnostic system for research of rotating machine parts vibration (in Czech), *Dynamika strojů* 2009, Praha : Ústav termomechaniky AV ČR, v.v.i., 2009, p.97–106
- [2] Procházka P., Vaněk F., Pešek L., Cibulka J., Vaněk P.: Inductive sensor for sensing position of rotating machine parts (in Czech), Utility model application: PUV 2009-21775.
- [3] Procházka P., Vaněk F., Pešek L., Cibulka J., Vaněk P.: Magnetoresistive sensor for sensing position of rotating machine parts (in Czech), Utility model application: PUV 2009-21776
- [4] Procházka P., Vaněk F., Pešek L., Cibulka J., Vaněk P. : A technology of contactless vibrodiagnostics of blades of steam turbines low-pressure parts (in Czech), Knowledge of research and development RIV/61388998—/07: 00309252, 2008
- [5] Vaněk F., Pešek L., Procházka P., Vaněk P., Cibulka J.: Vibrodiagnostic systems for dynamic parameter measurement of rotating parts in power industry (in Czech), Proc. of the conference Parní turbíny a jiné turbostroje 2007, Plzeň: A.S.I-Turbostroje Plzeň, Škoda Power a.s., Západočeská univerzita v Plzni, FST, KKE, 2007 p. 23/1–23/8
- [6] Daněk O., Vaněk F., Procházka P., Kozánek J., Pešek L.: Diagnostic Magneto-Kinetic Equipment MK3, Book of Abstracts – Identification and Updating Methods of Mechanical Structures – EUROMECH 437, Praha : Ústav termomechaniky AV ČR, 2002, p. 12, ISBN 80-85918-73-0

*Received in editor's office:* March 23, 2010

*Approved for publishing:* June 4, 2010

*Note:* This paper is an extended version of the contribution presented at the national colloquium with international participation *Dynamics of Machines 2010* in Prague.